Inorg. Chem. **2003**, *42*, 4773–4781

Inorganic Chemistry Article

Density Functional Theory Investigation of the Active Site of [Fe]-Hydrogenases: Effects of Redox State and Ligand Characteristics on Structural, Electronic, and Reactivity Properties of Complexes Related to the $[2Fe]_H$ Subcluster

Maurizio Bruschi,[†] Piercarlo Fantucci,[‡] and Luca De Gioia*,[‡]

Department of Environmental Sciences and Department of Biotechnology and Biosciences, University of Milan-Bicocca, Piazza della Scienza 2, I-20126 Milan, Italy

Received November 26, 2002

The effects of redox state and ligand characteristics on structural, electronic, and reactivity properties of complexes related to the $[2Fe]_H$ subcluster of [Fe]-hydrogenases have been investigated by DFT calculations and compared with experimental and theoretical data obtained investigating both the enzyme and synthetic model complexes. Our results show that $Fe^{II}Fe^{II}$ species characterized by OH or H_2O groups terminally coordinated to the iron atom distal to the terminal sulfur ligand (Fe^d) are less stable than corresponding μ-OH or μ-H_2O species, suggesting that the latter are destabilized or kinetically inaccessible in the enzyme. In addition, results obtained investigating Fe^IFe^I and $Fe^{II}Fe^I$ complexes show that structure and relative stability of species characterized by a μ-CO group are significantly affected by the electronic properties of the ligands coordinated to the iron atoms. The investigation of reaction pathways for H_2 activation confirms and extends a previous hypothesis indicating that H_2 can be cleaved on $Fe^{II}Fe^{II}$ species. In particular, even though [Fe]-hydrogenases are proposed to bind and activate H_2 at a single iron center, the comparison of our data with experimental results obtained studying synthetic complexes (Zhao, X.; Georgakaki, I. P.; Miller, M. L.; Mejia-Rodriguez, R.; Chiang, C.-Y.; Darensbourg, M. Y. *Inorg. Chem.* **2002**, *41*, 3917) suggests that activation paths involving both metal ions are also possible. Moreover, μ-H $Fe^{II}Fe^I$ complexes are predicted to correspond to stable species and might be formed in the enzyme catalytic cycle.

Introduction

[Fe]-hydrogenases are metalloproteins that catalyze the reversible oxidation of dihydrogen according to the reaction $H_2 \rightarrow 2H^+ + 2e^-$.[1] Recently, the X-ray structure of [Fe]-hydrogenases from the anaerobic microorganism *Clostridium pasteurianum*[2] (CpI) and the sulfate-reducing microorganism *Desulfovibrio desulfuricans*[3] (DdH) have been reported. The active site (the so-called H cluster) is formed by a regular $[Fe_4S_4]$ cluster, bridged by a cysteine residue to the $[2Fe]_H$ subcluster, where two iron atoms are coordinated by CO and CN^- ligands and bridged by a chelating $S-X_3-S$ group.[4] The $S-X_3-S$ ligand was initially described as 1,3-propanedithiol (PDT),[3] but other combinations of C, N, or O atoms would be consistent with the crystallographic data. Indeed, a recent X-ray reinvestigation of the [Fe]-hydrogenase from *D. desulfuricans*[5] has led to the proposal that the $S-X_3-S$ ligand is bis(thiomethyl)amine (DTMA). The $[2Fe]_H$ subcluster is the likely site of H_2 activation. Moreover, the X-ray-derived coordination environment of Fe^d (from hereafter Fe^p and Fe^d refer to proximal and distal iron atoms with respect to the terminal sulfur ligand, respectively), where a coordination position is vacant in DdH and occupied by a water molecule or an hydroxyl group in CpI, suggests that this could be the H_2 binding site (see Figure 1a).

* To whom correspondence should be addressed. E-mail: luca.degioia@unimib.it. Fax: +39.02.64483478.
† Department of Environmental Sciences.
‡ Department of Biotechnology and Biosciences.

(1) Albracht, S. P. J. *Biochim. Biophys. Acta* **1994**, *90*, 167−204. Adams, M. W. W. *Biochim. Biophys. Acta* **1990**, *1020*, 115−145.
(2) Peters, J. W.; Lanzilotta, W. N.; Lemon, B. J.; Seefeldt, L. C. *Science* **1998**, *282*, 1853−1858.
(3) Nicolet, Y.; Piras, C.; Legrand, P.; Hatchikian, E. C.; Fontecilla-Camps, J. C. *Structure* **1999**, *7*, 13−23.
(4) Peters, J. W. *Curr. Opin. Struct. Biol.* **1999**, *9*, 670−676. Nicolet, Y.; Lemon, B. J.; Fontecilla-Camps, J. C.; Peters, J. W. *Trends Biochem. Sci.* **2000**, *25*, 138−143.
(5) Nicolet, Y.; de Lacey, A. L.; Vernède, X.; Fernandez, V. M.; Hatchikian, E. C.; Fontecilla-Camps, J. C. *J. Am. Chem. Soc.* **2001**, *123*, 1596−1601.

10.1021/ic0262132 CCC: $25.00
Published on Web 06/27/2003

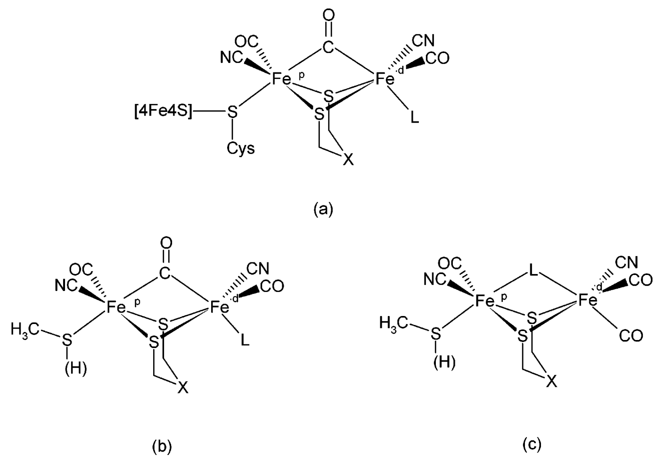

Figure 1. (a) Schematic representation of the $[2Fe]_H$ subcluster in [Fe]-hydrogenases as determined by X-ray diffraction. X can be either CH_2 or NH, and L is H_2O or OH^-. (b, c) Schematic representation of the $[2Fe]_H$ computational models investigated in this study. X can be CH_2 or NH, and L is a small group. Fe^p and Fe^d refer to proximal and distal iron atoms with respect to the CH_3S ligand, respectively.

Three redox states of the $[2Fe]_H$ subcluster have been well characterized by spectroscopic techniques.[3,6] The fully oxidized and reduced forms of the enzyme are EPR silent and should correspond to $Fe^{II}Fe^{II}$ and $Fe^{I}Fe^{I}$ redox states, respectively. The partially oxidized form is paramagnetic and should correspond to $Fe^{II}Fe^{I}$. When the enzyme is isolated in air, the H cluster is in the fully oxidized form and is catalytically inactive.[6e] However, Kubas and co-workers[7] reported H_2 activation on electrophilic organometallic complexes, suggesting that the heterolytic cleavage of H_2 in [Fe]-hydrogenases takes place on a low-spin Fe(II) center. Additionally, theoretical data suggest that the $Fe^{II}Fe^{II}$ $[2Fe]_H$ subcluster can heterolytically cleave H_2.[8,9] In fact, when H_2 binds terminally to the Fe^d center and the $S-X_3-S$ ligand is assumed to be a PDT moiety, the reaction is kinetically or thermodynamically hindered.[8] However, if DTMA is assumed to be the bridging ligand, the central N atom may act as a base in H_2 activation (see Figure 1a).[9] Very recently, a detailed theoretical investigation of models of the $[2Fe]_H$ subcluster where the $S-X_3-S$ ligand is DTMA has been reported,[10] confirming previous results[9] and suggesting that the oxidized form of the $[2Fe]_H$ subcluster is an $Fe^{II}Fe^{II}$ species with a hydroxyl group terminally coordinated to Fe^d. In addition, the presence of a CO group bridging the two Fe atoms was proposed to be crucial to stabilize the low oxidation states of the $[2Fe]_H$ subcluster. These computational investigations[8-10] were based on the structure of the $[2Fe]_H$ subcluster as observed in the X-ray structure of the enzyme and accordingly started from the assumption that H_2 is terminally coordinated to Fe^d. However, experimental[12-14] and DFT studies[8,11] of complexes related to the $[2Fe]_H$ subcluster revealed some unexpected structural and electronic characteristics of the bimetallic center. In particular, we have shown that, when considering $Fe^{II}Fe^{II}$ species,[11] complexes characterized by a bridging CO are almost as stable as corresponding species featuring only terminal CO ligands. Interestingly, it has been recently proposed, on the basis of experimental and computational data,[13] that the enzyme might play a crucial role in stabilizing forms of the $[2Fe]_H$ cluster characterized by a μ-CO group. In addition, H_2 can bind to Fe^p and its activation, involving both iron atoms and one of the bridging sulfur ligands, is associated with a very low activation energy, leading to intermediate species characterized by a μ-H atom. Remarkably, the X-ray structures of μ-$HFe^{II}Fe^{II}$ species related to the $[2Fe]_H$ subcluster have been recently reported.[14] These observations prompted us to investigate, by means of DFT calculations, the effect of redox state and ligand characteristics on structural and electronic properties of complexes related to the $[2Fe]_H$ subcluster characterized by bridging and terminal CO groups and PDT and DTMA chelating groups. On the ground of these results we have investigated also structural, electronic, and reactivity properties of species possibly involved in H_2 binding and activation.

Methods

Computational models of the $[2Fe]_H$ cluster are characterized by the general structure $[(\mu\text{-}Y)Fe_2(CO)_3(CN)_2(CH_3S)(L)]$ or $[(\mu\text{-}Y)Fe_2(CO)_3(CN)_2(CH_3SH)(L)]$ (where Y is PDT or DTMA and L is a small ligand) (see Figure 1b,c).

DFT calculations were carried out using the hybrid B3LYP exchange-correlation functional[15] and the effective atomic core potential derived by Hay and Wadt[16] for iron and sulfur atoms. The adopted basis set is of augmented double-ζ type: one set of f (exponent 0.800) and one set of d (exponent 0.540) polarization functions were added to Fe and S atoms, respectively.[17] All other atoms are described with the double-ζ D95V basis set.[18] For the reactive hydrogen atoms and the oxygen atom of H_2O, the D95V basis set was augmented by a set of standard p and d polarization functions, respectively.

(6) (a) Pierik, A. J.; Hagen, W. R.; Redeker, J. S.; Wolbert, R. B. G.; Boersma, M.; Verhagen, M. F. J. M.; Grande, H. J.; Veeger, C.; Mutsaers, P. H.; Sand, R. H.; Dunham, W. R. *Eur. J. Biochem.* **1992**, *209*, 63–71. (b) Patil, D. S.; Moura, J. J. G.; He, S. H.; Teixeira, M.; Prickril, B. C.; Der Vartanian, D. V.; Peck, H. D., Jr.; Legall, J.; Huyanh, B. H. *J. Biol. Chem.* **1988**, *263*, 18732. (c) De Lacey, A. L.; Stadler, C.; Cavazza, C.; Hatchikian, E. C.; Fernandez, V. M. *J. Am. Chem. Soc.* **2000**, *122*, 11232. (d) Chen, Z.; Lemon, B. J.; Huang, S.; Swartz, D. J.; Peters, J. W.; Bagley, K. A. *Biochemistry* **2002**, *41*, 2036. (e) Pierik, A. J.; Hulstein, M.; Hagen, W. R.; Albracht, S. P. *Eur. J. Biochem.* **1998**, *258*, 572.

(7) Huhmann-Vincent, J.; Scott, B. L.; Kubas, G. J. *Inorg. Chim. Acta* **1999**, *294*, 240–247.

(8) Cao, Z.; Hall, M. B. *J. Am. Chem. Soc.* **2001**, *123*, 3734–3742.

(9) Fan, H.-J.; Hall, M. B. *J. Am. Chem. Soc.* **2001**, *123*, 3828–3829.

(10) Liu, Z.-P.; Hu, P. *J. Am. Chem. Soc.* **2002**, *124*, 5175.

(11) Bruschi, M.; Fantucci, P.; De Gioia, L. *Inorg. Chem.* **2002**, *41*, 1421.

(12) (a) Lyon, E. J.; Georgakaki, I. P.; Reibenspies, J. H.; Darensbourg, M. Y. *Angew. Chem., Int. Ed.* **1999**, *38*, 3178–3180. (b) Schmidt, M.; Contakes, S. M.; Rauchfuss, T. B. *J. Am. Chem. Soc.* **1999**, *121*, 9736–9737. (c) Le Cloiret, A.; Best, S. P.; Borg, S.; Davies, S. C.; Evans, D. J.; Hughes, D. L.; Pickett, C. J. *Chem. Commun.* **1999**, *22*, 2285–2286.

(13) Lyon, E. J.; Georgakaki, I. P.; Reibenspies, J. H.; Darensbourg, M. Y. *J. Am. Chem. Soc.* **2001**, *123*, 3268.

(14) Zhao, X.; Georgakaki, I. P.; Miller, M. L.; Mejia-Rodriguez, R.; Chiang, C.-Y.; Darensbourg, M. Y. *Inorg. Chem.* **2002**, *41*, 3917.

(15) Becke, A. D. *Phys. Rev. A* **1988**, *38*, 3098–3104. Becke, A. D. *J. Chem. Phys.* **1992**, *96*, 2155–2160. Becke, A. D. *J. Chem. Phys.* **1993**, *98*, 5648–5652. Stevens, P. J.; Devlin, F. J.; Chablowski, C. F.; Frisch, M. J. *J. Phys. Chem.* **1994**, *98*, 11623–11627.

(16) Hay, P. J.; Wadt, W. R. *J. Chem. Phys.* **1985**, *82*, 299–306.

(17) Rassolov, V.; Pople, J. A.; Ratner, M.; Windus, T. L. *J. Chem. Phys.* **1998**, *109*, 1223. Check, C. E.; Faust, T. O.; Bailey, J. M.; Wright B. J.; Gilbert, T. M.; Sunderlin, L. S. *J. Phys. Chem. A* **2001**, *105*, 8111.

(18) Dunning, H., Jr.; Hay, P. J. In *Methods of Electronic Structure Theory*; Schaefer, H. F., III, Ed.; Plenum Press: New York, 1977; Vol. 3.

Stationary points of the energy hypersurface have been located by means of energy gradient techniques. In particular, transition state structures have been searched using the syncronous transit quasi-Newton method,[19] as implemented in the Gaussian 98 set of programs.[20] A full vibrational analysis has been carried out to further characterize each stationary point. Partial atomic charges have been computed according to the natural atomic orbital scheme.[21]

The optimized structures of the complexes reported in this study correspond always to low spin states, as expected considering the characteristics of the ligands forming the coordination environment of the metal atoms and in agreement with available experimental data.

Changes in the oxidation state of the proximal [Fe_4S_4] cluster observed in [Fe]-hydrogenases was simply modeled by varying the protonation state of the CH_3S ligand, following previous works by Hall and co-workers.[8]

Results and Discussion

1. Structural and Electronic Properties of Complexes Related to the [2Fe]$_H$ Subcluster. *$Fe^{II}Fe^{II}$ Model Complexes.* On the basis of X-ray data[2,3,5] and DFT calculations,[8,10] the [2Fe]$_H$ subcluster in the enzyme isolated in air should correspond to an $Fe^{II}Fe^{II}$ complex characterized by a μ-CO group and by a hydroxyl group or a water molecule terminally bound to Fe^d. To further investigate the characteristics of this species we have initially optimized and compared two possible isomers of [(μ-PDT)$Fe_2(CO)_3(CN)_2$(CH_3S)(OH)]$^{2-}$: the first resembling the $Fe^{II}Fe^{II}$ form of the [2Fe]$_H$ subcluster (**1**) and the second corresponding to an $Fe^{II}Fe^{II}$ complex characterized by a μ-OH group and by a terminal CO (**2**) (see Figure 2). Following previous proposals,[8,11] the CH_3S group was deprotonated to simulate the reduced redox state of the proximal [Fe_4S_4] cluster. The geometry features of **1** well compare with the corresponding X-ray data collected for the oxidized form of the enzyme, where a CO group bridges the two Fe ions.[2] In fact, in **1** the CO group is bridged in a symmetric fashion (Fe–C = 1.982 and 1.988 Å) and the Fe–Fe distance is equal to 2.57 Å. In **2**, the Fe–S bond distances are significantly longer than in **1** (see Figure 2) and the Fe–Fe distance is as long as 3.02 Å. The electronic characteristics of **1** and **2** are also very different, with electron density shifting from Fe^p to Fe^d going from **1** to **2** (see Table 1). If energies are considered, isomer **2** is more stable than **1** by 19.9 kcal mol^{-1}. The same stability trend was observed investigating analogous complexes where a water molecule replaces the hydroxyl group ($\Delta E = 9.7$ kcal mol^{-1}),[11] indicating that hydroxo and water ligands prefer a bridged position in the isolated $Fe^{II}Fe^{II}$ cluster. This observation is remarkable because it suggests that steric and/or electronic properties of the protein play a role in destabilizing or make kinetically inaccessible the μ-OH form of the $Fe^{II}Fe^{II}$ [2Fe]$_H$ subcluster within the enzyme.

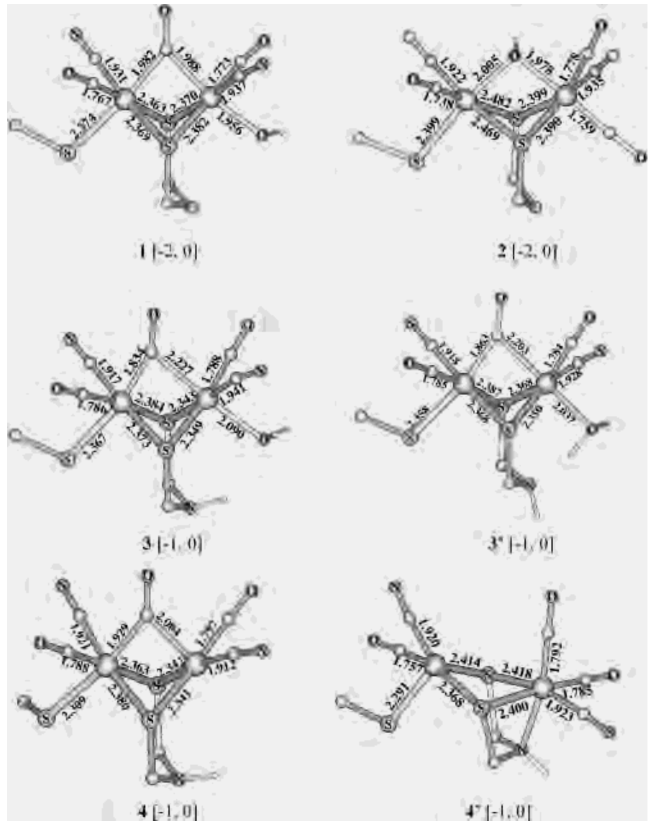

Figure 2. DFT-optimized structures of $Fe^{II}Fe^{II}$ model complexes are shown with their charge (*q*) and spin (*S*), [*q*, *S*]. Only the most relevant bond distances are explicitly shown. Fe–Fe distances for **1**–**3**, **3′**, **4**, and **4′** are 2.568, 3.023, 2.570, 2.579, 2.515, and 3.327 Å, respectively.

It has been recently suggested that a DTMA ligand, instead of PDT, bridges the two Fe atoms in the [2Fe]$_H$ subcluster, and DFT calculations on [Fe]-hydrogenase models containing DTMA have been reported.[9,10] However, the effects of the chelating group on the structural and electronic characteristics of the bimetallic cluster have not yet been thoroughly investigated. The optimized structures of two isomers of [(μ-DTMA)$Fe_2(CO)_3(CN)_2(CH_3S)(H_2O)$]$^-$, differing for the configuration of the N atom of DTMA, are shown in Figure 2 (**3** and **3′**) and are very similar to the previously published corresponding species where PDT substitutes DTMA,[11] the only notable difference being the hydrogen bond formed by the NH group of DTMA with the water molecule coordinated to Fe^d. As expected, **3** and **3′** are very close in energy, **3′** being more stable by only 3.7 kcal mol^{-1}. Similar considerations hold true when comparing [(μ-DTMA)$Fe_2(CO)_3(CN)_2(CH_3S)(OH)$]$^{2-}$ isomers and the corresponding PDT complex (data not shown). On the other hand, the optimized structures of [(μ-DTMA)$Fe_2(CO)_3(CN)_2(CH_3S)$]$^-$ isomers (**4** and **4′**; see Figure 2), which can be considered the products of H_2O loss from **3** and **3′**, respectively, are extremely different. In particular, in the $Fe^{II}Fe^{II}$ species **4′**, the N atom of DTMA is coordinated to Fe^d (N–Fe^d = 2.042

(19) Peng, C.; Schlegel, H. B. *Isr. J. Chem.* **1994**, *33*, 449–458.
(20) Frisch, M. J.; Trucks, G. W.; Schlegel, H. B.; Scuseria, G. E.; Robb, M. A.; Cheeseman, J. R.; Zakrzewski, V. G.; Montgomery, J. A., Jr.; Stratmann, R. E.; Burant, J. C.; Dapprich, S.; Millam, J. M.; Daniels, A. D.; Kudin, K. N.; Strain, M. C.; Farkas, O.; Tomasi, J.; Barone, V.; Cossi, M.; Cammi, R.; Mennucci, B.; Pomelli, C.; Adamo, C.; Clifford, S.; Ochterski, J.; Petersson, G. A.; Ayala, P. Y.; Cui, Q.; Morokuma, K.; Malick, D. K.; Rabuck, A. D.; Raghavachari, K.; Foresman, J. B.; Cioslowski, J.; Ortiz, J. V.; Stefanov, B. B.; Liu, G.; Liashenko, A.; Piskorz, P.; Komaromi, I.; Gomperts, R.; Martin, R. L.; Fox, D. J.; Keith, T.; Al-Laham, M. A.; Peng, C. Y.; Nanayakkara, A.; Gonzalez, C.; Challacombe, M.; Gill, P. M. W.; Johnson, B. G.; Chen, W.; Wong, M. W.; Andres, J. L.; Head-Gordon, M.; Replogle, E. S.; Pople, J. A. *Gaussian 98*; Gaussian, Inc.: Pittsburgh, PA, 1998.
(21) Reed, A. E.; Weinstock, R. B.; Weinhold, F. J. *J. Chem. Phys.* **1985**, *83*, 735.

Table 1. Natural Atomic Charges of Diamagnetic $Fe^{II}Fe^{II}$ and $Fe^{I}Fe^{I}$ Complexes[g]

	1[a]	2[a]	3[a]	4[a]	5[b]	6[b]	7[b]	14[a,c]	16[a,c]	17[a,c]	18[a]	20[a]
Fe^p	−0.20	0.15	−0.24	0.11	−0.15	−0.02	−0.29	−0.24	−0.23	−0.17	−0.12	−0.19
Fe^d	0.00	−0.14	0.12	−0.16	−0.24	−0.25	−0.27	0.11	−0.26	−0.34	−0.34	−0.32
S_t	−0.21[d]	−0.34[d]	−0.13[d]	−0.21[d]	0.15[e]	−0.37[d]		−0.14[d]	−0.17[d]	−0.27[d]	−0.31[d]	0.18[e]
S_b	−0.02	−0.09	−0.08	−0.05	−0.12	−0.13	−0.03	−0.03	0.00	0.25[f]	−0.06	−0.02
S_b	−0.04	−0.10	−0.08	−0.09	−0.15	−0.19	−0.05	−0.01	0.07	−0.01	−0.03	−0.05
H_b										−0.04	−0.05	−0.01

[a] $Fe^{II}Fe^{II}$ complexes. [b] $Fe^{I}Fe^{I}$ complexes. [c] Data from ref 11. [d] CH_3–S ligand. [e] CH_3–SH ligand. [f] Protonated sulfur atom. [g] S_b and H_b stand for bridging sulfur and hydrogen atoms, respectively. S_t stands for the sulfur atom terminally coordinated to Fe^p. Natural atomic charges for **3′** and **4′** are extremely similar to the values computed for **3** and **4**, respectively, and therefore are not reported.

Å) and is trans to a CO group, resulting in a distorted octahedral Fe^d environment. On the other side, in **4** the configuration of the NH group of DTMA does not allow the formation of the N−Fe bond. Remarkably, **4′** is more stable than **4** by about 22 kcal mol^{-1}. In addition, the computed reaction energy for **3** → **4** + H_2O is as large as 20.0 kcal mol^{-1}, similarly to the corresponding reaction energy computed when PDT replaces DTMA (25.0 kcal mol^{-1}).[11] However, the reaction energy for **3′** → **4′** + H_2O is as low as 1.7 kcal mol^{-1}, a value that becomes even favorable if energy contributions deriving from hydrogen bonds involving the displaced water molecule and **4′** are kept into account (data not shown), suggesting that the N atom of DTMA can compete with a water molecule for Fe^d coordination. Moreover, H_2 cannot easily displace the intramolecularly coordinated N atom of DTMA in **4′**, the reaction being endothermic by about 4 kcal mol^{-1} (L. De Gioia, unpublished data). However, it is relevant to underline that the NH bond of DTMA may form a hydrogen bond with a nearby deprotonated cysteine in the enzyme and this interaction may lessen the interaction of the N atom with the iron center.

Fe^IFe^I Model Complexes. As the second step of this investigation, we turned our attention to Fe^IFe^I complexes, which have been extensively investigated by experimental[12] and theoretical[8,10] approaches, showing that the reduced redox state of the $[2Fe]_H$ subcluster is compatible with an Fe^IFe^I species. Moreover, it has been suggested that the structure of the Fe^IFe^I $[2Fe]_H$ subcluster is stabilized by the enzyme in a conformation more similar to a transition state associated to FeL_3 unit rotation rather than to the ground-state structure observed in related Fe^IFe^I synthetic complexes.[13] With the aim of investigating how slight changes in the nature of Fe ligands may affect the structure of Fe^IFe^I species, we have investigated $[(\mu\text{-PDT})Fe_2(CO)_3(CN)_2(CH_3SH)]^{2-}$ (**5**) and $[(\mu\text{-PDT})Fe_2(CO)_3(CN)_2(CH_3S)]^{3-}$ (**6**), which differ only for the protonation state of the CH_3S ligand. In both structures (see Figure 3), one of the CO groups coordinated to Fe^d bends toward Fe^p and interacts, albeit slightly, with the metal ion, as deduced by the observed rotation of the Fe^dL_3 unit and by the value of the Fe^d−C−O angle, which is lower than 180° (173.0 and 163.5° in **5** and **6**, respectively). The Fe^p−C distance is equal to 2.883 and 2.638 Å in **5** and **6**, respectively. Analysis of atomic charges shows that Fe^p is more electron rich in **5** (−0.15) than in **6** (−0.02), despite the larger total negative charge of the latter. Remarkably, the atomic charge of the C atom belonging to the semibridged

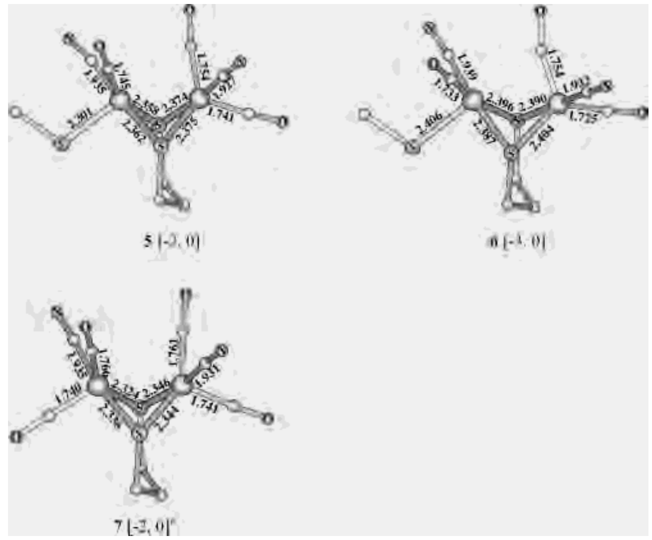

Figure 3. DFT-optimized structures of Fe^IFe^I model complexes are shown with their charge (q) and spin (S), [q, S]. Only the most relevant bond distances are explicitly shown. Fe−Fe distances for **5**−**7** are 2.528, 2.655, and 2.555 Å, respectively. Superscript a indicates data are from ref 11.

CO decreases significantly going from **5** (0.49) to **6** (0.39). These observations suggest that a significant back-donation from Fe^p to the semibridging CO is operative in **6**. To further investigate the effect of Fe ligands on the structure of Fe^I-Fe^I species, we have compared the DFT structure of $[(\mu\text{-PDT})Fe_2(CO)_4(CN)_2]^{2-}$ (complex **7**; see Figure 3), which was already shown to well reproduce the corresponding experimental structure,[11] with **5**, **6**, and $[(\mu\text{-PDT})Fe_2(CO)_6]$, whose DFT structure was reported by Hall et al.[8] The comparison reveals that the bending toward Fe^p of one CO group coordinated to Fe^d, and consequently the rotation of the Fe^dL_3 unit, increase in the order $[(\mu\text{-PDT})Fe_2(CO)_6]$, $[(\mu\text{-PDT})Fe_2(CO)_4(CN)_2]^{2-}$ (**7**), $[(\mu\text{-PDT})Fe_2(CO)_3(CN)_2(CH_3SH)]^{2-}$ (**5**), and $[(\mu\text{-PDT})Fe_2(CO)_3(CN)_2(CH_3S)]^{-3}$ (**6**) and are correlated to the total charge of the complex and to the electron-donor characteristics of the Fe^p ligands (CO, CN, CH_3SH, CH_3S; see also Table 1); the more electron-donating the ligand coordinated to Fe^p, the more effective the back-donation from Fe^p to the semibridging CO and, consequently, the more rotated is the Fe^dL_3 unit. Analogous results were obtained with DTMA complexes (data not shown). Therefore, structures characterized by a semibridged CO correspond to stable energy minima when suitable electron-donor ligands are coordinated to Fe^p. These observations suggest also that the tuning of electron density on Fe^p, which in the enzyme could be achieved by oxidation−reduction of the $[Fe_4S_4]$ cluster, may act as a switch stabilizing either μ- or terminal CO

Table 2. Natural Atomic Charges and Spin Densities (in Parentheses) of Paramagnetic $Fe^{II}Fe^{I}$ Complexes[a]

	8	**9**	**10**	**11**	**12**	**13**	**15**	**19**	**21**	**22**
Fe^p	−0.16 (0.08)	−0.15 (0.09)	0.31 (1.73)	0.15 (0.73)	−0.25 (0.49)	−0.08 (−0.10)	−0.12 (0.02)	−0.03 (0.89)	−0.08 (0.00)	−0.15 (0.03)
Fe^d	0.03 (0.97)	0.02 (0.99)	−0.18 (−0.49)	−0.23 (0.29)	0.02 (0.37)	0.06 (1.14)	−0.06 (0.86)	−0.36 (0.20)	−0.04 (0.89)	−0.06 (0.87)
S_t	0.19[b] (0.01)	−0.26[c] (0.02)	0.02[b] (0.06)	−0.35[c] (0.01)	0.27[b] (0.07)	0.22[b] (0.00)	0.20[b] (0.01)	0.00[b] (0.04)	−0.25[c] (0.01)	−0.35[c] (−0.01)
S_b	−0.10 (0.02)	−0.11 (−0.01)	−0.13 (−0.03)	−0.09 (−0.04)	−0.09 (0.03)	−0.15 (−0.03)	−0.14 (0.02)	0.20[d] (0.02)	−0.17 (0.00)	0.13[d] (0.01)
S_b	−0.09 (−0.01)	−0.12 (−0.02)	−0.07 (−0.01)	−0.06 (0.02)	−0.10 (0.02)	−0.20 (0.10)	-0.08 (0.00)	−0.10 (0.00)	−0.11 (0.01)	−0.08 (−0.02)
H_b								−0.03 (−0.09)		−0.12 (−0.02)
$\langle S^2\rangle$[e]	0.7961	0.7875	1.3248	0.9057	0.8220	0.8420	0.7861	0.7915	0.7786	0.7805

[a] S_b and H_b stand for bridging sulfur and hydrogen atoms, respectively. S_t stands for the sulfur atom terminally coordinated to Fe^p. [b] CH_3−S ligand. [c] CH_3−SH ligand. [d] Protonated sulfur atom. [e] Expectation value of the squared spin operator before annihilation. The spin projection technique applied to spin-unrestricted wave function led to mainly pure doublet state (0.75), with the exception of **10**, which is contaminated by high-spin contributions.

forms. In fact, the structures of **5** and **6**, both characterized by a semibridging CO group, are extremely similar to the structure of the $[2Fe]_H$ subcluster observed within the enzyme poised to the reduced redox state, supporting the crystallographic and FTIR spectroscopic evidence for changes in Fe coordination upon reduction of the active site.[5] In particular, C−Fe^d and C−Fe^p distances in the Fe^IFe^I complex **6** are 1.754 and 2.638 Å, respectively, and are very similar to the experimental values (1.69, 2.4/2.56 Å [5] or 1.8, 2.6 Å [3]).

$Fe^{II}Fe^{I}$ Model Complexes. Modification of the Fe coordination environment observed as a function of metal redox state and nature of its ligands prompted us to extend the investigation also to Fe^IFe^{II} species. This redox state should correspond to the partially reduced and EPR-active form of the $[2Fe]_H$ subcluster and could be involved in the catalytic cycle of the enzyme. In particular, DFT calculations[8,10] have shown that, in $Fe^{II}Fe^{I}$ species, a CO group can bridge the two iron atoms, resulting in a vacant coordination position on Fe^d where H_2 can bind (see Figure 1b). However, little is known about structure and stability of $Fe^{II}Fe^{I}$ species characterized by nonbridging CO groups.

As for Fe^IFe^I species, we have carried out calculations on complexes characterized by CH_3S ($[(\mu\text{-PDT})Fe_2(CO)_3(CN)_2(CH_3S)]^{2-}$) and CH_3SH ($[(\mu\text{-PDT})Fe_2(CO)_3(CN)_2(CH_3SH)]^{-}$) Fe^p ligands. Remarkably, for both complexes we have obtained two isomers, characterized by bridging (**8** and **9**) and nonbridging (**10** and **11**) CO groups, respectively (see Figure 4). In **8**, the CO group bridges the two Fe atoms in a nonsymmetric fashion (Fe^p−C = 2.116 Å; Fe^d−C = 1.878 Å) and the Fe−Fe distance is 2.582 Å. In its isomer **10**, the Fe ions are both five-coordinated and the Fe−Fe distance is equal to 2.559 Å. The SH−Fe^p bond distance increases by more than 0.2 Å going from **8** to **10** (2.336 Å in **8** and 2.575 Å in **10**). This bond length, and to a lesser extent the Fe−CO and Fe−CN bond distances, are correlated to the electron density on the Fe^p atom (see Table 2), which is lower in **8** due to back-donation from Fe^p to the bridging CO group. Population analysis (see Table 2) shows that in **8** the spin density is largely localized on Fe^d. On the other side, **10** is a spin-polarized complex with large spin density on both Fe^p (1.73) and Fe^d (−0.49). Isomers **8** and **10** are almost isoenergetic (**8** → **10**; $\Delta E = -0.93$ kcal mol^{-1}).

In the dianionic complex **9**, one CO bridges the two Fe ions in an almost symmetric fashion (see Figure 4; Fe^p−CO = 2.017 Å, Fe^d−CO = 1.952 Å). The shortening of the Fe^p−CO bond with respect to **8** is due to the substitution of CH_3SH with CH_3S, causing an increased back-donation from Fe^p to the bridging CO. In **9**, the unpaired electron is almost completely localized on Fe^d (see Table 2) and the computed energy values show that also **9** and **11** are almost isoenergetic (**9** → **11**; $\Delta E = 3.62$ kcal mol^{-1}), even though in this case the μ-CO form is more stable.

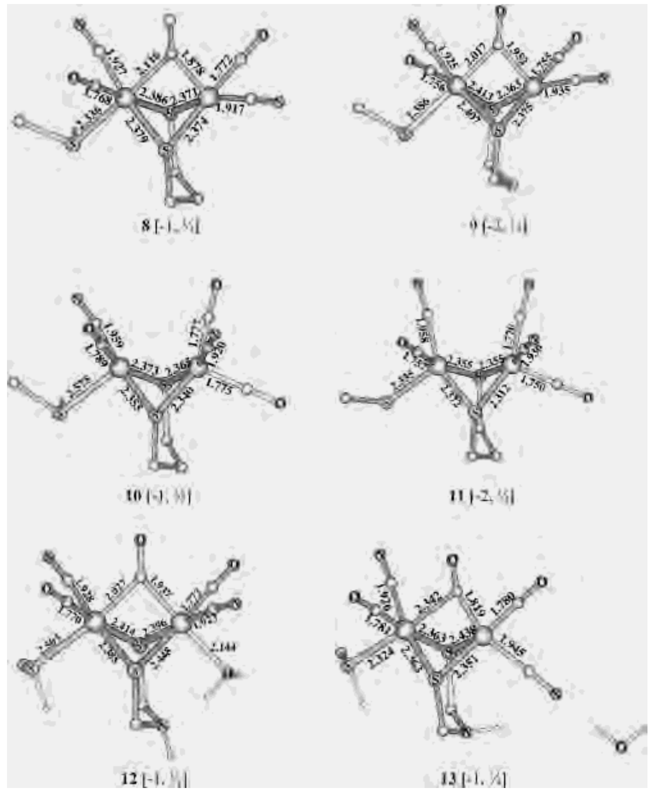

Figure 4. DFT-optimized structures of $Fe^{II}Fe^{I}$ model complexes are shown with their charge (q) and spin (S), [q, S]. Only the most relevant bond distances are explicitly shown. Fe−Fe distances for **8**−**13** are 2.582, 2.597, 2.559, 2.587, 2.681, and 2.582 Å, respectively.

In **11**, the two Fe atoms are five-coordinated and the Fe−Fe distance is equal to 2.587 Å. The comparison with **10** (see Figure 4) reveals that the only geometry feature significantly affected by the protonation state of the CH_3S ligand is the CH_3S−Fe^p bond distance, as expected. On the other side, the electronic properties are affected in a more subtle way (see Table 2). The strong spin polarization reported for **10** is not observed in **11**, where the spin density is unevenly distributed between Fe^p (0.73) and Fe^d (0.29) (see Table 2). It is also remarkable that in the case of the μ-CO complexes **8** and **9**, Fe^d is more electrophilic than Fe^p, whereas the reverse is true in the case of the nonbridged

Scheme 1. Plausible Catalytic Cycle for Dihydrogen Activation Where the H_2 Cleavage Step Takes Place on a Formally $Fe^{II}Fe^{II}$ Redox Species (R = CH_3) with Energy Differences (in kcal mol^{-1}) Associated with Relevant Reaction Steps Reported[a]

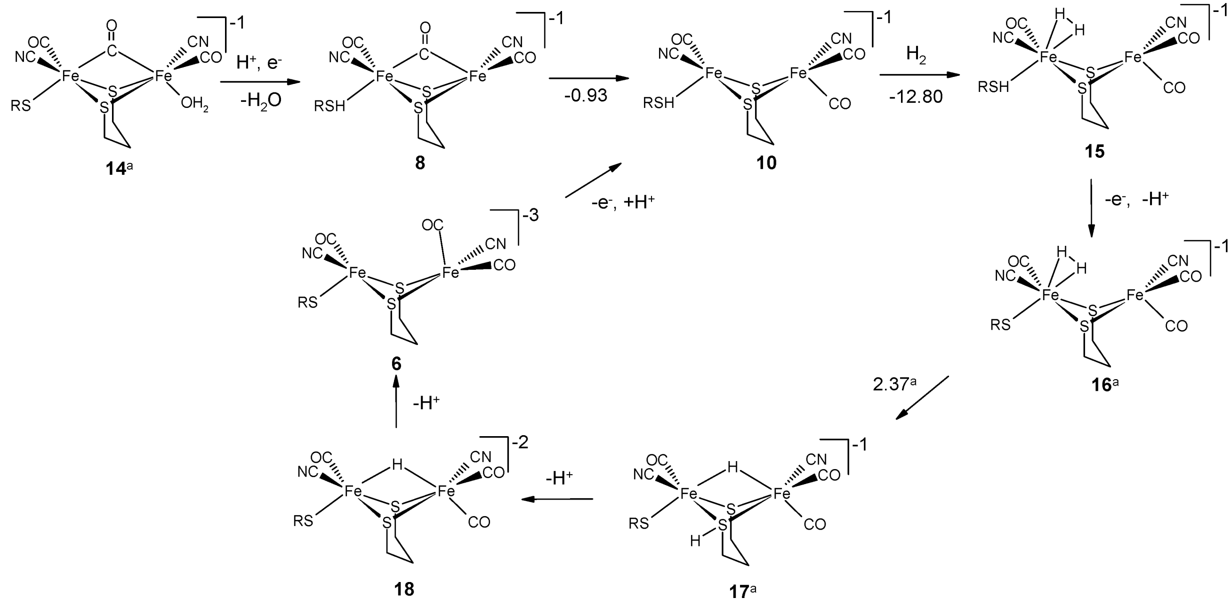

[a] Structures and energy difference from ref 11.

complexes **10** and **11**. This observation is relevant to better understand H_2 binding to these complexes (see below).

In previous DFT investigations, carried out on $Fe^{II}Fe^{I}$ models characterized by a PDT ligand,[8] it was shown that a H_2O molecule cannot bind to Fe^d, leaving a coordination position vacant to bind H_2. Similar results were obtained investigating $Fe^{II}Fe^{I}$ computational models characterized by a DTMA ligand.[10] However, isomers differing for the configuration of the NH group of DTMA have not yet been investigated. Indeed, the orientation of the NH group with respect to Fe^d can significantly affect the structural and electronic properties of these complexes, as shown above for $Fe^{II}Fe^{II}$ species. To further investigate these aspects we have carried out geometry optimization of $[(\mu\text{-DTMA})Fe_2(CO)_3(CN)_2(CH_3SH)(H_2O)]^-$ isomers differing for the configuration of the NH group (**12** and **13**; see Figure 4). Remarkably, in **12** the H_2O molecule remains coordinated to Fe^d (Fe^d–O = 2.144 Å), due to the formation of a H-bond between the N atom of DTMA and the water molecule. In **13**, where the N–H bond has an axial orientation, the water molecule moves away from Fe^d, resulting in an adduct where the CN^- group coordinated to Fe^d rearranges forming one H-bond with the NH group and the H_2O molecule. Considering relative stabilities, it turns out that **12** is less stable than **13** by 6.5 kcal mol^{-1}. These results prompted us to investigate also the product of H_2O loss from **12**: $[(\mu\text{-DTMA})Fe_2(CO)_3(CN)_2(CH_3SH)]^-$. Remarkably, during DFT optimization, Walden inversion of the N atom of DTMA was observed, leading to a structure of the bimetallic cluster that very closely resembles that observed in **13**. However, the observation that the removal of H_2O from **12** results in an energy minimum structure resembling **13** does not necessarily imply a low-energy transition state along this reaction path. Moreover, it should be noted that hydrogen bonds between the CN^- group and the protein may abolish the rearrangement of Fe^d coordination environment observed in **13**.

2. H_2 Activation on $[2Fe]_H$ Model Complexes. On the basis of X-ray data[2,3] and DFT calculations,[9] it has been suggested that dihydrogen activation in [Fe]-hydrogenases implies binding of H_2 to the Fe^d center and heterolytic cleavage possibly mediated by the N atom of the chelating DTMA ligand. However, the data discussed in section 1 indicate that when considering computational models of the isolated $[2Fe]_H$ subcluster, a facile conversion between species characterized by bridged and terminal CO is possible, indirectly suggesting the possibility of different H_2 binding mode. Moreover, previous theoretical investigations predicted the existence of $Fe^{II}Fe^{II}$ species characterized by a H atom bridging the two metal centers, suggesting possible alternative pathways for H_2 activation.[8,11] Indeed, recent experimental investigations have shown that ligands with better donor ability than CO promote the binuclear oxidative addition of H^+ to yield $[Fe^{II}(\mu\text{-H})Fe^{II}]$ species.[14]

To further explore some of these aspects and evaluate their relevance to enzymatic and synthetic systems, we have investigated intermediate species and transition states that imply H_2 activation leading to μ-H intermediate species. In the reaction paths investigated we have always assumed as starting point the $[(\mu\text{-PDT})Fe_2(CO)_3(CN)_2(CH_3S)(H_2O)]^-$ species, which is similar to the oxidized form of the $[2Fe]_H$ subcluster observed in the enzyme. In addition, a sulfur atom of PDT has been assumed to be involved in the heterolytic H_2 cleavage. The implications of these assumptions are discussed, in light of computational results, in the final section of the paper.

H_2 Activation on $Fe^{II}Fe^{II}$ Species. Considering as starting point the $Fe^{II}Fe^{II}$ species $[(\mu\text{-PDT})Fe_2(CO)_3(CN)_2(CH_3S)(H_2O)]^-$ (**14**; see Scheme 1), whose structure and electronic

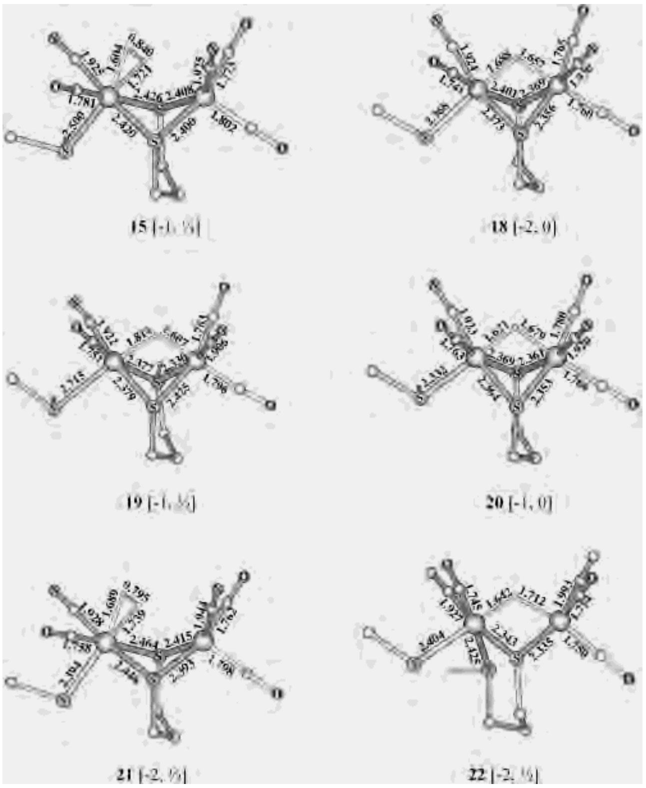

Figure 5. DFT-optimized structures of models of the $[2Fe]_H$ subcluster that may have relevance in H_2 activation are shown with their charge (*q*) and spin (*S*), [*q*, *S*]. Only the most relevant bond distances are explicitly shown. Fe−Fe distances for **15** and **18**−**22** are 2.960, 2.651, 2.811, 2.588, 3.215, and 2.803 Å, respectively.

properties were already reported;[11] the first step for the activation of the bimetallic cluster is the freeing of a coordination position to bind H_2, most probably associated with the dissociation of the water molecule (or hydroxyl group) coordinated to Fe^d. However, previous DFT calculations[8,11] have shown that this step is largely endothermic when considering $Fe^{II}Fe^{II}$ species, whereas the monoelectron reduction of the cluster to an Fe^IFe^{II} species makes the water dissociation favorable.[8] According to these considerations, the $Fe^{II}Fe^I$ species $[(\mu\text{-PDT})Fe_2(CO)_3(CN)_2(CH_3SH)]^-$ (**8**) (see Scheme 1) is the first product formed by monoelectron reduction of **14** (and H_2O loss). It should be noted that the CH_3S ligand in **8** is protonated, to mimic the concomitant oxidation of the proximal $[Fe_4S_4]$ cluster. The structures of **14** and **8** are similar except for the position of the μ-CO group, which moves toward Fe^d going from **14** to **8** (Fe^d−CO = 2.233 and 1.878 Å in **14** and **8**, respectively). Comparison of partial atomic charge values (Tables 1 and 2) reveals a less pronounced Fe^p−Fe^d polarization in **8** with respect to **14**. The coordinatively unsaturated species **8** can rearrange to species **10** (see Scheme 1). As stated above, **8** and **10** are almost isoenergetic and their interconversion is expected to be a facile process.[22] **10** can bind H_2 to the electrophilic Fe^p (see Table 2) forming **15** (see Figure 5; ΔE for **10** + H_2 → **15** = −12.80 kcal mol^{-1}), where dihydrogen is slightly activated, as deduced by comparison of the H−H bond lengths in **15** (0.840 Å) and in the isolated H_2 molecule computed using the same method and basis set (0.734 Å). Upon H_2 binding the Fe−Fe distance increases by almost 0.4 Å, whereas the other structural features remain similar to those observed in **10**. However, electron density and spin distribution are very sensitive to the binding of H_2. In fact, the electronic properties of **15** are markedly different from those observed in the precursor **10** and resemble those observed in **8** (see Table 2).

According to a reaction path where H_2 activation is promoted by an $Fe^{II}Fe^{II}$ species, it must be assumed, in agreement with Hall and co-workers,[8] that the $Fe^{II}Fe^I$ species **15** is oxidized to **16** (see Scheme 1), whose DFT structure was previously reported.[11] Following the assumptions made initially, the simultaneous reduction of the proximal $[Fe_4S_4]$ cluster is mimicked by deprotonation of the CH_3S ligand coordinated to Fe^p. The geometry rearrangement observed in the reaction **15** → **16** is negligible, except for the expected decrease of the Fe^p−CH_3S bond distance. In a previous DFT study[11] we have shown that H_2 activation starting from the $Fe^{II}Fe^{II}$ species **16** is kinetically and thermodynamically favorable (ΔE = 2.37 kcal mol^{-1}; $\Delta E^‡$ = 5.34 kcal mol^{-1}), leading to a species (**17**) characterized by a μ-H atom bridging the two iron centers.[11] **17** can release one H^+ (see Scheme 1) forming the intermediate species **18**, where a μ-H atom is still present (see Figure 5). Then, **18** loses another H^+ forming the Fe^IFe^I species **6**, which closely resembles the structure of the $[2Fe]_H$ subcluster as observed in the reduced form of the enzyme. Finally, **6** loses one electron closing the catalytic cycle (see Scheme 1).

H_2 Activation on an Fe^IFe^{II} Species. As discussed above, H_2 can be heterolytically cleaved on $Fe^{II}Fe^{II}$ species. To investigate the possibility that the $Fe^{II}Fe^I$ complex **15** can heterolytically cleave dihydrogen (see Scheme 2), without assuming previous monoelectron oxidation of the $Fe^{II}Fe^I$ adduct, we have computed the structure of **19** (see Figure 5), which is the product of H_2 cleavage starting from the Fe^IFe^{II} complex **15**. In **19**, a hydrogen atom bridges asymmetrically the two metal centers, being closer to Fe^d, whereas the other H atom is bonded to one of the PDT sulfur atom. Interestingly, as in the case of the analogous $Fe^{II}Fe^{II}$ species **17**,[11] the protonation of the S atom does not preclude its coordination to the two metal centers. Considering electronic properties, it is interesting to note that, in **19**, Fe^d is electron richer than Fe^p, whereas the spin density is almost completely localized on Fe^p (see Table 2). Considering relative energies, it turns out that the **15** → **19** step is endothermic by 9.34 kcal mol^{-1}. The potential energy surface was sampled to locate the transition state structure along this crucial reaction step. However, despite using different initial guess structures, we were not able to locate any chemically reasonable structure corresponding to a saddle point on the potential energy surface. In particular, release of HCN from the complex was often observed.

To close the catalytic cycle the $Fe^{II}Fe^I$ species **19** should release one proton and one electron, forming **20** (see Figure 5), which differs from **18** only for the protonation state of the terminal S ligand. The structures of **18** and **20** are very

(22) Cotton, F. A.; Wilkinson, G. *Advanced Inorganic Chemistry*, 5th ed.; John Wiley and Sons: New York, 1995.

Scheme 2. Plausible Catalytic Cycle for Dihydrogen Activation Where the H_2 Cleavage Step Takes Place on a Formally $Fe^{II}Fe^{I}$ Redox Species (R = CH_3) and the RSH Terminal Ligand Remains Protonated along All the Catalytic Cycle with Energy Differences (in kcal mol^{-1}) Associated with Relevant Reaction Steps Reported

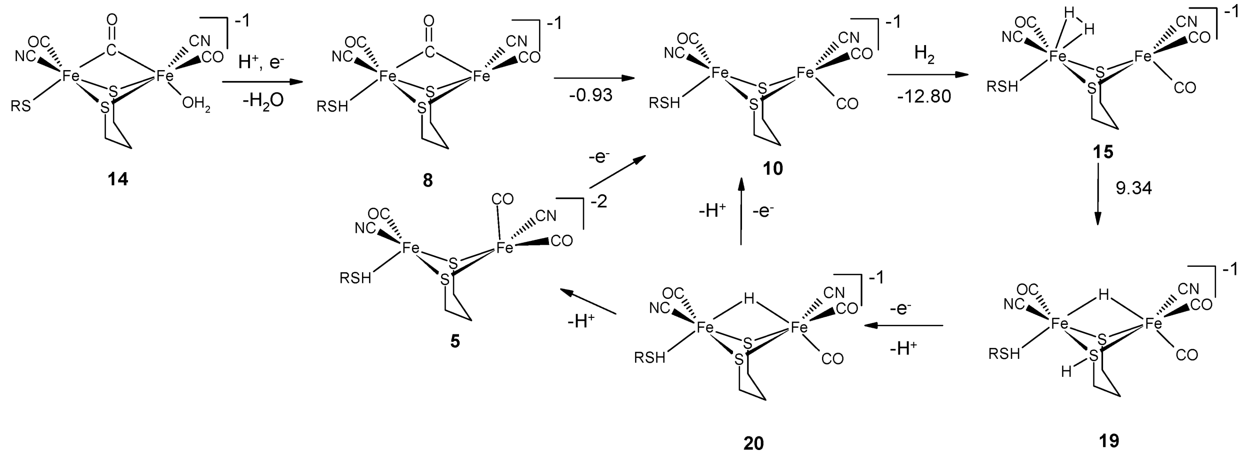

Scheme 3. Plausible Catalytic Cycle for Dihydrogen Activation Where the H_2 Cleavage Step Takes Place on a Formally $Fe^{II}Fe^{I}$ Redox Species (R = CH_3) and the RS Terminal Ligand Remains Deprotonated along All the Catalytic Cycle with Energy Differences (in kcal mol^{-1}) Associated with Relevant Reaction Steps Reported

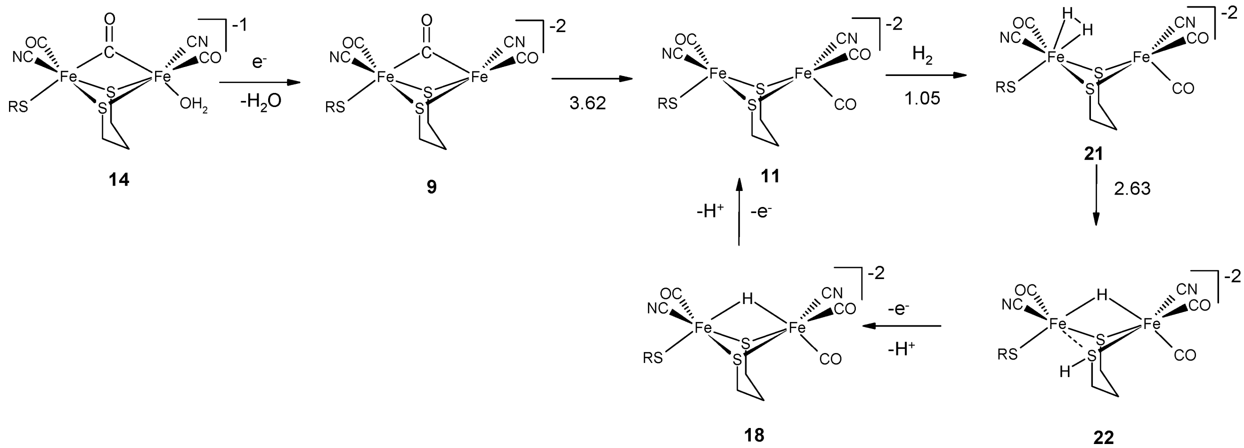

similar and both feature a symmetric Fe−H−Fe bridge, similarly to related synthetic complexes.[14] Also the electronic properties of **18** and **20** are quite similar (see Table 1) and, interestingly, Fe^d is electron richer than Fe^p, despite the coordination to the latter of a $CH_3S(H)$ ligand instead of a CO group. **20** can loose a H^+ forming **5**, which resembles the fully reduced structure of the active site and closes the catalytic cycle by monoelectron oxidation.

The subtle modulation of the electronic and structural properties of the cluster due to the different protonation of the terminal CH_3S ligand prompted us to investigate also a reaction path where dihydrogen is still activated on an Fe^{II}-Fe^{I} species but the terminal CH_3S ligand remains deprotonated through all the catalytic cycle (see Scheme 3). According to this path, the reductive activation of the Fe^{II}-Fe^{II} species **14** leads to **9**, which can rearrange to **11** in a slightly endothermic step (see above). **11** is still able to bind H_2 to Fe^p forming **21** (see Figure 5). However, the reaction **11** + H_2 → **21** is slightly endothermic (ΔE = 1.05 kcal mol^{-1}) and significantly less favored than the corresponding **10** + H_2 → **15** step. Remarkably, the Fe^p center in **10** is significantly more electrophilic than in **11** (see Table 2). In addition, the H−H bond distance in **21** is shorter (0.795 Å) than in **15** (0.840 Å). Moreover, natural bond orbital analysis[21] reveals that in **15** the occupations for σ and σ^* H_2 orbitals are 1.68 and 0.08, respectively, whereas in **21** the corresponding values are 1.74 and 0.08. These data suggest that σ-donation from the H−H bond to the metal is the most important contribution to the Fe^p−H_2 bond, whereas back-donation from the metal to H_2 plays a less important role. Indeed, H_2 binding and heterolysis is usually favored when H_2 is coordinated to relatively electron-rich metal centers and it is in trans to π-acceptor ligands such as CO, whereas donor ligands should favor oxidative addition of H_2 to form dihydride species.[23] However, due to the electrophilic nature of Fe^p in **10** and **11**, the H_2 bonding is mainly governed by σ-donation even in the presence of donor ligands coordinated to the iron center.

The comparison of the $Fe^{II}Fe^{I}$ dianionic species **21** with the monoanionic species **15** (see Figure 5) reveals also that, besides the expected longer CH_3SH−Fe^p bond distance observed in **15**, the Fe^p−Fe^d distance increases by more than 0.25 Å going from **15** to **21**. H_2 activation on **21** leads to **22** in a reaction step endothermic by only 2.63 kcal mol^{-1}.

(23) Kubas, G. J. *Metal Dyhydrogen and σ-Bond Complexes*; Kluwer Academic/Plenum Press: New York, 2001.

However, also in this case attempts to locate transition state structures characterized by incipient formation of S−H bonds were unsuccessful due to release of HCN from the complex.

It is also interesting to note that structures and electronic properties of possible products of H_2 cleavage involving the S atoms of PDT in $Fe^{II}Fe^{I}$ species are strongly influenced by the protonation state of the terminal S ligand, as judged by the comparison of species **22** and **19** (see Figure 5). In fact, in the dianionic complex **22**, the protonation of a PDT sulfur atom results in the cleavage of the SH−Fe^{d} bond, which is maintained in the monoanionic complex **19**. Also the spin density distribution is very different, the unpaired electron being localized on Fe^{p} and Fe^{d} in **19** and **22**, respectively. To close the catalytic cycle (see Scheme 3), **22** should loose one electron and one proton forming **18**, which, by subsequent release of one proton and one electron, forms **11**.

Conclusions

The effects of redox state and ligand characteristics on structural, electronic, and reactivity properties of model complexes related to the $[2Fe]_H$ subcluster of [Fe]-hydrogenases have been investigated by DFT calculations and compared with experimental and computational data, derived investigating both [Fe]-hydrogenases and model complexes, resulting in a better understanding of the chemical properties of the bimetallic cluster. In particular, the following observations can be offered: (i) $Fe^{II}Fe^{II}$ species characterized by OH or H_2O groups terminally coordinated to Fe^{d}, as observed in the X-ray structure of the enzyme, are less stable than corresponding μ-OH or μ-H_2O species, suggesting that the latter are destabilized or kinetically inaccessible in the enzyme. (ii) The structure of $Fe^{I}Fe^{I}$ species is strongly affected by the electronic properties of Fe^{p} and consequently by the chemical nature of its ligands. Electron donor ligands such as CH_3S^- (which closely mimic the cysteinate residue bridging Fe^{p} and the $[Fe_4S_4]$ cluster in the enzyme) lead to semibridging CO species very similar to the structure of the $[2Fe]_H$ subcluster as observed in the fully reduced state of the enzyme. (iii) For $Fe^{I}Fe^{II}$ species, terminal and μ-CO isomers are very close in energy, suggesting that both forms could be relevant in the catalytic cycle of the enzyme. (iv) Finally, the replacement of PDT with DTMA may have some influence on the structural properties of the bimetallic cluster.

We have also investigated the heterolytic cleavage of H_2 mediated by $[2Fe]_H$ models, confirming and extending previous hypothesis indicating that dihydrogen can be activated on $Fe^{II}Fe^{II}$ species. Moreover, even though [Fe]-hydrogenases are proposed to bind and activate H_2 at a single iron center, the comparison of computational and experimental[13] data obtained investigating model complexes suggests that reaction paths involving both metal ions are also possible. Our results indicate also that μ-H $Fe^{II}Fe^{I}$ complexes correspond to low-energy stable species, suggesting that they could play a role in the catalytic cycle.

Acknowledgment. The authors thank G. Zampella and the anonymous reviewers for their fruitful comments.

IC0262132